

Acoustical-Mode-Driven Electron-Phonon Coupling in Transition-Metal Diborides

Prabhakar P. Singh*

Department of Physics, Indian Institute of Technology, Powai, Mumbai- 400076, India

We show that the electron-phonon coupling, $\lambda_{\mathbf{q}\nu}$, in the transition-metal diborides NbB_2 and TaB_2 is dominated by the longitudinal acoustical (LA) mode, in contrast to the optical E_{2g} mode dominated coupling in MgB_2 . Our *ab initio* results, described in terms of phonon dispersion, linewidth, and $\lambda_{\mathbf{q}\nu}$ along $\Gamma - A$, also show that (i) NbB_2 and TaB_2 have a relatively weak electron-phonon coupling, (ii) the E_{2g} linewidth is an order of magnitude larger in MgB_2 than in NbB_2 or TaB_2 , (iii) the E_{2g} frequency in NbB_2 and TaB_2 is considerably higher than in MgB_2 , and (iv) the LA frequency at A for TaB_2 is almost half of that of MgB_2 or NbB_2 .

The discovery of superconductivity in MgB_2 [1, 2] has renewed interests [3, 4, 5, 6, 7, 8, 9, 10, 11] in finding superconductivity in similar materials such as simple metal diborides (BeB_2 , $BeB_{2.75}$ [3]), transition-metal diborides (NbB_2 [4, 5], TaB_2 [4, 6], MoB_2 [7], ZrB_2 [8]), borocarbides ($LiBC$ [9, 10]), and other alloys [11]. Surprisingly, many of the materials mentioned above have not shown any superconductivity, those who are found to superconduct do so at a relatively low $T_c < 10 K$, and very likely, require hole doping and/or external pressure to show superconductivity. For example, the recent work of Yamamoto *et al.* [4] showing superconductivity in hole-doped Nb_xB_2 is a case in point. Thus, of all the diborides, MgB_2 seems to be in a class by itself with a $T_c = 39 K$ while all the other diborides have $T_c < 10 K$.

Recent work on MgB_2 [12, 13, 14, 15, 16, 17, 18, 19, 20] have unambiguously shown a very strong and anisotropic electron-phonon coupling in this system. In particular, it is found that electron/hole states on the cylindrical sheets of the Fermi surface along $\Gamma - A$ couple very strongly to the in-plane $B - B$ bond stretching E_{2g} phonon mode [15, 16, 17, 18, 19]. The E_{2g} phonon mode coupling gives rise to partial electron-phonon coupling constant $\lambda_{\mathbf{q}\nu}$ of the order of 2 – 3 [19]. Such a large partial $\lambda_{\mathbf{q}\nu}$ along $\Gamma - A$ results in a relatively high superconducting transition temperature of 39 K. Thus, the observed differences in the superconducting properties of MgB_2 *vis-a-vis* other diborides, specially the transition-metal diborides, can be better understood by comparing the electron-phonon coupling along $\Gamma - A$ in these systems. Taking the cue, we have studied from first principles (i) the phonon dispersion $\omega_{\mathbf{q}\nu}$, (ii) the phonon linewidth $\gamma_{\mathbf{q}\nu}$ [21], and (iii) the partial electron-phonon coupling constant $\lambda_{\mathbf{q}\nu}$ along $\Gamma - A$ in MgB_2 , NbB_2 and TaB_2 in $P6/mmm$ crystal structure.

We have calculated the electronic structure of MgB_2 , NbB_2 and TaB_2 in $P6/mmm$ crystal structure. We used optimized lattice constants a and c for MgB_2 and NbB_2 [20], and experimental lattice constants ($a = 5.826 a.u.$, $c = 6.130 a.u.$) for TaB_2 which are close to our optimized values of $a = 5.792 a.u.$ and $c = 6.143 a.u.$. The lattice constants were optimized using the ABINIT program [22] based on pseudopotentials and plane waves.

For studying the electron-phonon interaction we used the full-potential linear response program of Savrasov [23, 24] to calculate the dynamical matrices and the Hopfield parameter, which were then used to calculate the phonon dispersion $\omega_{\mathbf{q}\nu}$, the phonon linewidth $\gamma_{\mathbf{q}\nu}$, and the partial electron-phonon coupling constant $\lambda_{\mathbf{q}\nu}$ along $\Gamma - A$ in MgB_2 , NbB_2 and TaB_2 .

Based on our calculations, described below, we find that (i) in contrast to a strong and E_{2g} -mode dominated electron-phonon coupling in MgB_2 , the transition-metal diborides NbB_2 and TaB_2 have a relatively weak electron-phonon coupling which is dominated by the longitudinal acoustical (LA) mode, (ii) the E_{2g} phonon linewidth is an order of magnitude larger in MgB_2 than in NbB_2 or TaB_2 , and (iii) the E_{2g} phonon frequency in NbB_2 as well as TaB_2 is considerably higher than in MgB_2 while the LA phonon frequency at A for TaB_2 is almost half of that of MgB_2 or NbB_2 .

Before describing our results in detail, we provide some of the computational details. As indicated above, the structural relaxation was carried out by the molecular dynamics program ABINIT [22] with Broyden-Fletcher-Goldfarb-Shanno minimization technique using Troullier-Martins pseudopotential [25] for MgB_2 and Hartwigsen-Goedecker-Hutter pseudopotentials [26] for NbB_2 and TaB_2 , 512 Monkhorst-Pack [27] \mathbf{k} -points and Teter parameterization for exchange-correlation. The kinetic energy cutoff for the plane waves was 110 Ry for MgB_2 and 140 Ry for NbB_2 and TaB_2 . The charge self-consistent full-potential LMTO [23] calculations for electronic structure were carried out with the generalized gradient approximation for exchange-correlation of Perdew *et al* [28] and 484 \mathbf{k} -points in the irreducible wedge of the Brillouin zone. In these calculations, we used s , p , d and f orbitals at the Mg and Ta sites, and s , p and d orbitals at the Nb and B sites. The $2p$ state of Mg as well as the $5s$ and $5p$ states of Ta were treated as semi-core states. In all cases the potential and the wave function were expanded up to $l_{max} = 6$. The muffin-tin radii for Mg , B , Nb and Ta were taken to be 2.4, 1.66, 2.3 and 2.5 atomic units, respectively.

The calculation of dynamical matrices and the Hopfield parameters along $\Gamma - A$ were carried out for 4 equidis-

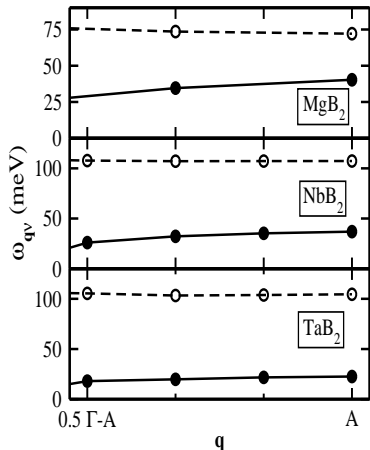


Figure 1: The phonon dispersion $\omega_{\mathbf{q}\nu}$ of MgB_2 (upper panel), NbB_2 (middle panel) and TaB_2 (lower panel) for longitudinal acoustical (solid circles connected with full line) and optical E_{2g} (open circles connected with dashed line) modes along $\Gamma-A$, calculated using the full-potential linear response method as described in the text. The lines connecting the points are only a guide to the eye.

Table I: The phonon frequencies (in meV) at Γ and A for the E_{2g} and the LA modes for MgB_2 calculated using the linear response method as described in the text as well as from previous work.

	$\omega_{\Gamma}(E_{2g})$	$\omega_A(E_{2g})$	$\omega_A(LA)$
Present work	78	72	40
Kong <i>et al.</i> [15]	73	71	38
Bohnen <i>et al.</i> [16]	71	63	39
Shukla <i>et al.</i> [19]	65	57	37

tant \mathbf{q} -points for MgB_2 and 7 equidistant \mathbf{q} -points for NbB_2 and TaB_2 . For Brillouin zone integrations we used a $12 \times 12 \times 12$ grid while the Fermi surface was sampled more accurately with a $36 \times 36 \times 36$ grid of \mathbf{k} -points using the double grid technique as outlined in Ref. [24]. We checked the convergence of the relevant quantities by carrying out Brillouin zone integrations using a $16 \times 16 \times 16$ grid of \mathbf{k} -points with Fermi surface sampling done over $48 \times 48 \times 48$ grid.

In Fig. 1 we show the phonon dispersion of MgB_2 , NbB_2 and TaB_2 for LA and optical E_{2g} modes along $\Gamma-A$. For MgB_2 , a comparison of our calculations of E_{2g} and LA phonon frequencies at Γ and A points with the previous calculations of Refs. [15, 16, 19] is given in Table I. As expected, our results are closer to the work of Ref. [15]. The difference in the E_{2g} phonon frequency at Γ , which has been found to be very sensitive to the

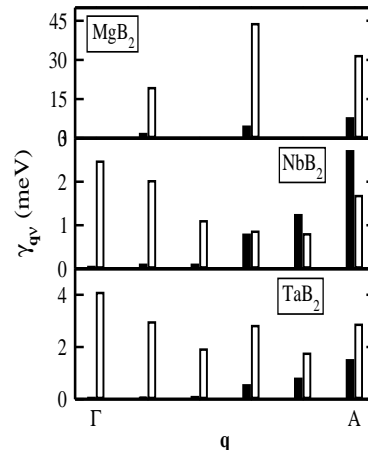


Figure 2: The phonon linewidth $\gamma_{\mathbf{q}\nu}$ of MgB_2 (upper panel), NbB_2 (middle panel) and TaB_2 (lower panel) for LA (solid bar) and optical E_{2g} (open bar) modes along $\Gamma-A$, calculated using the full-potential linear response method as described in the text. The phonon linewidth for the LA mode in MgB_2 has been multiplied by a factor of 10 for clarity.

structural input and Brillouin zone integration [16], arises due to the experimental lattice constants used in Refs. [15, 16, 19]. The value calculated by Shukla *et al.* for E_{2g} phonon frequency is somewhat lower. However, our calculated frequency for LA phonon mode at A is in good agreement with previous calculations. We expect $\omega_{\mathbf{q}\nu}$ for NbB_2 and TaB_2 to have similar accuracy.

In NbB_2 and TaB_2 , the E_{2g} phonon mode along $\Gamma-A$ has considerably stiffened in comparison with MgB_2 . The E_{2g} frequency in MgB_2 changes from 78 to 72 meV , while for NbB_2 and TaB_2 it changes from 110 to 107 meV and 108 to 105 meV from Γ to A , respectively. The E_{2g} frequency at Γ in TaB_2 , as calculated by Rosner *et al.* [29], is 98 meV . The LA phonon mode at A for TaB_2 (22 meV) is almost half of that of MgB_2 (40 meV) and NbB_2 (37 meV). Here, we like to point out that in the present work the number of \mathbf{q} points chosen along $\Gamma-A$ is not sufficient to say anything about the anomaly in the acoustical mode.

The differences in the nature of electron-phonon interaction between MgB_2 and the transition-metal diborides NbB_2 and TaB_2 become quite apparent if one considers the electron-phonon contribution to the phonon lifetimes. In the case of MgB_2 , as shown by Shukla *et al.* [19], the anharmonic effects [17, 18] make negligible contribution to the phonon linewidth. Thus, the anomalous broadening of the E_{2g} phonon linewidth along $\Gamma-A$ underscores the strength of the electron-phonon coupling for this particular mode in MgB_2 [19]. To see what hap-

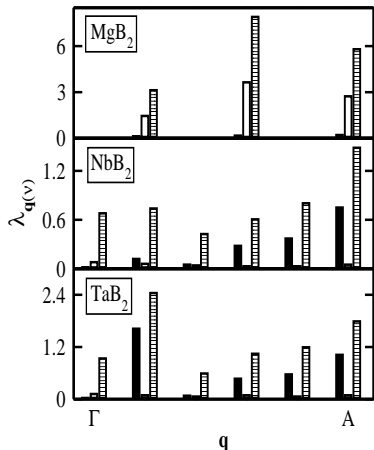


Figure 3: The partial electron-phonon coupling constant $\lambda_{\mathbf{q}\nu}$ of MgB_2 (upper panel), NbB_2 (middle panel) and TaB_2 (lower panel) for LA (solid bar) and optical E_{2g} (open bar) modes along $\Gamma - A$, calculated using the full-potential linear response method as described in the text. The total electron-phonon coupling constant $\lambda_{\mathbf{q}}$ (lined bar) is also shown.

pens in the transition-metal diborides, we show in Fig. 2 the phonon linewidths of MgB_2 , NbB_2 and TaB_2 for LA and E_{2g} modes along $\Gamma - A$. For MgB_2 , our calculated $\gamma_{\mathbf{q}\nu}$'s are in reasonable agreement with the results of Ref. [19]. Note that the values shown in Fig. 2 correspond to twice the linewidth. From Fig. 2, it is clear that in MgB_2 the electron-phonon coupling along $\Gamma - A$ is dominated by the optical E_{2g} phonon mode with a maximum $\gamma_{E_{2g}}$ of 44 meV , and that the LA mode plays essentially no role. In contrast, in NbB_2 and TaB_2 (i) the linewidths are more than an order of magnitude smaller than in MgB_2 , for example the maximum $\gamma_{E_{2g}}$ is only about 4 meV in TaB_2 and (ii) the contribution from the E_{2g} mode decreases from 4 to 2.8 meV , while that due to LA mode increases from 0.02 to 1.5 meV , as one moves from Γ to A . The phonon linewidths of MgB_2 and the transition-metal diborides NbB_2 and TaB_2 , as described above, clearly demonstrate the differences in the strength and the nature of electron-phonon interaction in these systems.

To see the strengths with which the LA and the E_{2g} phonon modes couple to the electrons, we show in Fig. 3 the partial as well as the total electron-phonon coupling constant ($\lambda_{\mathbf{q}}$) along $\Gamma - A$ for MgB_2 , NbB_2 and TaB_2 . Certainly, the most striking feature of these systems, as evidenced in Fig. 3, is the overall strength of the electron-phonon coupling in MgB_2 ($\lambda_{\mathbf{q}} \sim 7.9$) as compared to NbB_2 ($\lambda_{\mathbf{q}} \sim 1.5$) and TaB_2 ($\lambda_{\mathbf{q}} \sim 2.5$); nevertheless the additional feature of E_{2g} -dominated $\lambda_{\mathbf{q}}$

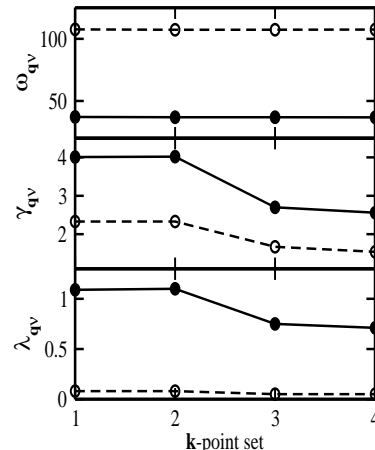


Figure 4: The convergence of $\omega_{\mathbf{q}\nu}$, $\gamma_{\mathbf{q}\nu}$, and $\lambda_{\mathbf{q}\nu}$ at A in the Brillouin zone for NbB_2 as a function of \mathbf{k} -points using the double-grid technique as described in the text. In the present case the four sets correspond to 50, 133, 133, and 270 irreducible \mathbf{k} -points for the electronic self-consistency and 793, 793, 2413, and 5425 irreducible \mathbf{k} -points for the Fermi surface sampling, respectively.

in MgB_2 giving way to LA -dominated $\lambda_{\mathbf{q}}$ in NbB_2 and TaB_2 is just as striking. Thus, the electron-phonon coupling in the transition-metal diborides NbB_2 and TaB_2 is essentially due to the LA mode (the transverse acoustical mode makes some contribution), the contribution from the E_{2g} mode being insignificant. For TaB_2 , Rosner *et al.* [29] also found $\lambda_{E_{2g}} = 0.05$ at Γ , in agreement with the present work. However, their [29] conclusion about the strength of the electron-phonon coupling in TaB_2 is erroneous because it doesn't take into account the contributions from the acoustical modes properly. We also note that, in our opinion [20, 30], the experimentally [31] deduced electron-phonon coupling in NbB_2 and TaB_2 are underestimated. These differences in the electron-phonon coupling between MgB_2 and the transition-metal diborides NbB_2 and TaB_2 may help explain why MgB_2 superconducts at 39 K while NbB_2 and TaB_2 do not show any superconductivity down to 2 K .

Finally, in Fig. 4 we show the convergence of $\omega_{\mathbf{q}\nu}$, $\gamma_{\mathbf{q}\nu}$, and $\lambda_{\mathbf{q}\nu}$ at A in the Brillouin zone for NbB_2 as a function of \mathbf{k} -points using the double-grid technique as outlined in Ref. [24]. The use of double-grid technique allows one to construct two separate but commensurate \mathbf{k} -grids, one for the electronic charge self-consistency and the other for Fermi-surface sampling. We employed 4 sets of double grids (i) (8, 8, 8, 24), (ii) (12, 12, 12, 24), (iii) (12, 12, 12, 36), and (iv) (16, 16, 16, 48), where the first three numbers define the electronic self-consistency grid and the last number sets up the Fermi-surface sampling

grid which is commensurate with the first grid. We find that the results are converged for the (12,12,12,36) grid used in the present work.

In conclusion, we have studied from first principles (i) the phonon dispersion, (ii) the phonon linewidth, and (iii) the partial electron-phonon coupling constant along $\Gamma - A$ in MgB_2 , NbB_2 and TaB_2 in $P6/mmm$ crystal structure. We find that (i) in contrast to a strong and E_{2g} -mode dominated electron-phonon coupling in MgB_2 , the transition-metal diborides NbB_2 and TaB_2 have a relatively weak electron-phonon coupling which is dominated by the LA mode, (ii) the E_{2g} phonon linewidth is an order of magnitude larger in MgB_2 than in NbB_2 or TaB_2 , and (iii) the E_{2g} phonon frequency in NbB_2 as well as TaB_2 is considerably higher than in MgB_2 while the LA phonon frequency at A for TaB_2 is almost half of that of MgB_2 or NbB_2 .

* Electronic address: ppsingh@phy.iitb.ac.in

- [1] J. Akimitsu, Symp. on Transition Metal Oxides, Sendai, January 10, 2001;
- [2] J. Nagamatsu *et al.*, Nature **410**, 63 (2001).
- [3] D. P. Young *et al.*, cond-mat/0104063 v4.
- [4] A. Yamamoto *et al.*, cond-mat/0208331.
- [5] J. Akimitsu, as cited in Ref. [4].
- [6] D. Kaczorowski *et al.*, cond-mat/0103571.
- [7] L. E. Muzzy *et al.*, cond-mat/0206006.
- [8] V. A. Gasparov *et al.*, JETP Lett. **73**, 532 (2001); cond-mat/0104323.
- [9] D. Souptel *et al.*, cond-mat/0208346 v2.
- [10] A. Bharathi *et al.*, cond-mat/0207448.
- [11] See references in Prabhakar P. Singh and P. Jiji Thomas Joseph, J. Phys.: Condens Matter **14**, 12441 (2002).
- [12] J. Kortus *et al.*, Phys. Rev. Lett. **86**, 4656 (2001).
- [13] J. M. An and W. E. Pickett, Phys. Rev. Lett. **86**, 4366 (2001).
- [14] Prabhakar P. Singh, Phys. Rev. Lett. **87**, 87004 (2001).
- [15] Y. Kong *et al.*, Phys. Rev. B **64** 20501 (2001).
- [16] K.-P. Bohnen *et al.*, Phys. Rev. Lett. **86**, 5771 (2001).
- [17] T. Yildirim *et al.*, Phys. Rev. Lett. **87**, 37001 (2001).
- [18] H. J. Choi *et al.*, cond-mat/0111182; cond-mat/0111183.
- [19] A. Shukla *et al.*, cond-mat/0209064.
- [20] Prabhakar P. Singh, cond-mat/0210091 (accepted for publication in Solid State Commun.).
- [21] P. B. Allen, Phys. Rev. B **6**, 2577 (1972).
- [22] <http://www.abinit.org/>.
- [23] S. Y. Savrasov, Phys. Rev. B **54**, 16470 (1996).
- [24] S. Y. Savrasov and D. Y. Savrasov, Phys. Rev. B **54**, 16487(1996).
- [25] N. Troullier and J. L. Martins, Phys. Rev. B **43**, 1993 (1991).
- [26] C. Hartwigsen *et al.*, Phys. Rev. B **58**, 3641 (1998).
- [27] H. J. Monkhorst and J. D. Pack, Phys. Rev. B **13**, 5188 (1976).
- [28] J. P. Perdew and Y. Wang, Phys. Rev. B **45**, 13244 (1992); J. Perdew *et al.*, Phys. Rev. Lett. **77**, 3865 (1996).
- [29] H. Rosner *et al.*, cond-mat/0106092.
- [30] Prabhakar P. Singh, unpublished.
- [31] Yu. G. Naiduk *et al.*, Phys. Rev. B **66**, 140301(R) (2002).